LAWRENCE
LIVERMORE
NATIONAL
LABORATORY

LLNL-PROC-680475

Progress in detailed modeling of DT implosion experiments on the National Ignition Facility

D. S. Clark

January 4, 2016

2015 Nuclear Explosives Design Physics Conference
Los Alamos, NM, United States
October 19, 2015 through October 23, 2015

Disclaimer

This document was prepared as an account of work sponsored by an agency of the United States government. Neither the United States government nor Lawrence Livermore National Security, LLC, nor any of their employees makes any warranty, expressed or implied, or assumes any legal liability or responsibility for the accuracy, completeness, or usefulness of any information, apparatus, product, or process disclosed, or represents that its use would not infringe privately owned rights. Reference herein to any specific commercial product, process, or service by trade name, trademark, manufacturer, or otherwise does not necessarily constitute or imply its endorsement, recommendation, or favoring by the United States government or Lawrence Livermore National Security, LLC. The views and opinions of authors expressed herein do not necessarily state or reflect those of the United States government or Lawrence Livermore National Security, LLC, and shall not be used for advertising or product endorsement purposes.

Progress in detailed modeling of DT implosion experiments on the National Ignition Facility (U)

D. S. Clark, C. R. Weber, D. C. Eder, S. W. Haan, B. A. Hammel, D. E. Hinkel, O. S. Jones, M. M. Marinak, J. L. Milovich, P. K. Patel, H. F. Robey, J. D. Salmonson, and S. M. Sepke

Lawrence Livermore National Laboratory, Livermore, California 94550, USA,

In order to achieve the several hundred Gbar stagnation pressures necessary for inertial confinement fusion ignition, implosion experiments on the National Ignition Facility (NIF) require the compression of deuterium-tritium fuel layers by a convergence ratio of approximately forty. Such high convergence implosions are subject to degradation by a range of perturbations, including the growth of small-scale defects due to hydrodynamic instabilities, as well as longer scale modulations due to radiation flux asymmetries in the enclosing hohlraum. Due to the broad range of scales involved, and also the genuinely 3-D character of the flow, accurately modeling NIF implosions remains at the edge of current simulation capabilities. This paper describes the current state of progress of 3-D, high-resolution, capsule-only simulations of NIF implosions aimed at accurately describing the performance of specific NIF experiments. Current simulations include the effects of hohlraum radiation asymmetries, capsule surface defects, the capsule support tent and fill tube, and use a grid resolution shown to be converged in companion two-dimensional simulations. The results of detailed simulations of low foot implosions from the National Ignition Campaign are contrasted against results for more recent high foot implosions. While the simulations suggest that low foot performance was dominated by ablation front instability growth, especially the defect seeded by the capsule support tent, high foot implosions appear to be dominated by hohlraum flux asymmetries, although the support tent still plays a significant role. Most importantly, it is found that a single, standard simulation methodology roughly captures the performance of both implosion types and gives confidence that such a model can be used to guide future implosion designs toward ignition. (Unclassified)

Introduction

Substantial progress has been made in modeling and understanding ignition implosions on the National Ignition Facility (NIF) in recent years. Specifically, hydrodynamic instability growth spectra have been measured for a range of perturbation mode numbers and for high foot as well as low foot implosion types [1]. These measurements have so far largely validated the simulation technique used to model NIF implosions, although measurements at higher convergence [2] and with better resolution are needed. In addition, the high foot implosion platform has been pushed to higher implosion velocities using higher laser powers and energies, and also thinner ablators, and appears to show evidence of a ceiling in performance. From the simulation perspective, detailed 3-D capsule-only simulations are showing increasing levels of agreement with NIF implosion measurements. In particular, these detailed simulations have now been compared for representative low foot [3] and high foot [4] implosion types, and show similar levels of agreement with the data for these quite different implosion types. This paper summarizes recent progress in 3-D simulations of NIF implosions using the radiation hydrodynamics code HYDRA [5]. The different implosion characteristics, as revealed in simulations of low as compared to high foot implosions, and their different failure modes are particularly important as these indicate where each implosion type may

be improved and how a route to ignition on NIF might finally be achieved.

3-D simulation results

3-D capsule-only simulations were run following the methodology described in Ref. [6]. Since the simulations in Ref. [6] were reported, further 2-D simulation work suggested that the perturbation seeded by the capsule support tent was even larger than assumed in those simulations. The understanding of the low-mode radiation flux asymmetries imprinted on the capsule from the hohlraum has also improved. For these reasons, the NIF implosion simulated in Ref. [6] (N120321, the highest compression implosion yet fired on NIF) was rerun with these updated inputs. Two additional implosion experiments have also been simulated: N120405, a higher power and energy companion to N120321 that "mixed" heavily with ~1 μg of ablator material believed to have entered the hot spot; and N130927, a high power high foot implosion that showed the first evidence of "fuel gain," that is, a fusion neutron yield equal to or greater than the peak fuel kinetic energy. It is important to understand the behavior of N120405 as it clearly crossed a performance "cliff" compared to N120321, and understanding the origin of this cliff—the source of the hot spot mix mass in particular—is essential in avoiding this outcome in future implosions. It is equally important to contrast the results of the low foot implosions (N120321 and N120405) against the high foot to understand the different strengths, and weaknesses, of these quite different implosion types.

Figure 1 contrasts the results from 3-D simulations of each of these shots at their respective bang times (time of peak neutron production). In each case, the outer surface is the ablation front colored by the electron temperature, the left cutaway shows the ion temperature, and the right cutaway shows the density. The large "sombrero hat" features in both of the low foot implosions result from ablation front instability growth seeded by the capsule support tent. As is clear from the figure, the tent is the dominant perturbation in these low foot implosions. In fact, in the case of N120405, it can be seen that the tent perturbation has grown so extreme that it has entrained plastic ablator material into the center of the hot spot. This appears to explain the source of the hot spot mix mass observed for this shot: the stronger acceleration and hence ablation front instability growth of N120405 amplified the tent perturbation to such an extent that the already large perturbation on N120321 grew to the point of penetrating the hot spot on N120405. Note that the tent perturbation encircles the full azimuth of the capsule at each pole and hence gives a large area for ablator material to enter the hot spot suddenly once an amplitude threshold is passed. In contrast, the

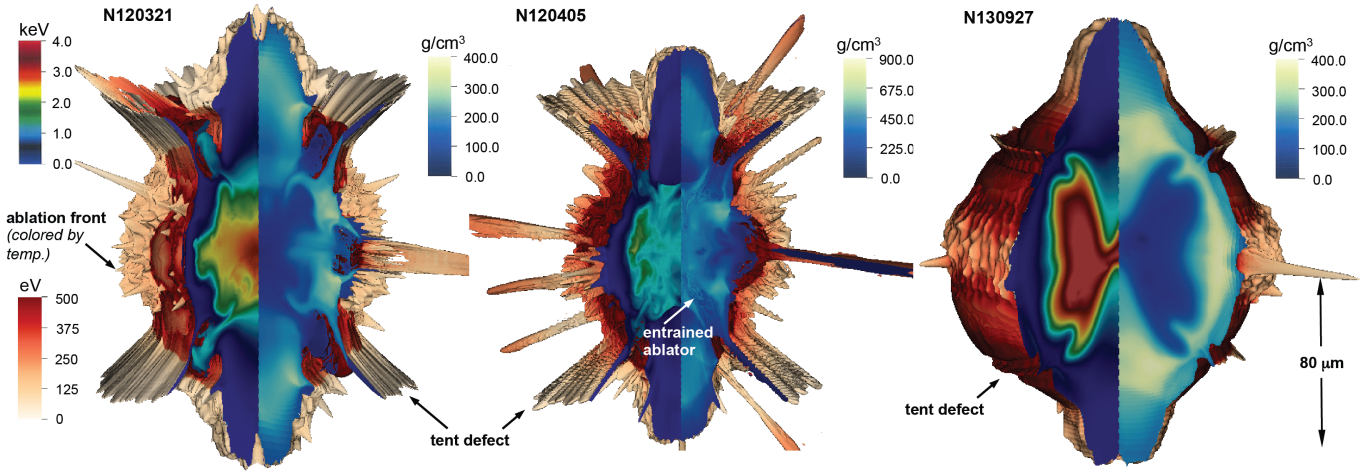

Fig. 1. Comparison of 3-D simulation results for N120321, N120405, and N130927 at their respective bang times. Temperature color scales are the same between all three simulations but the density scales differ.

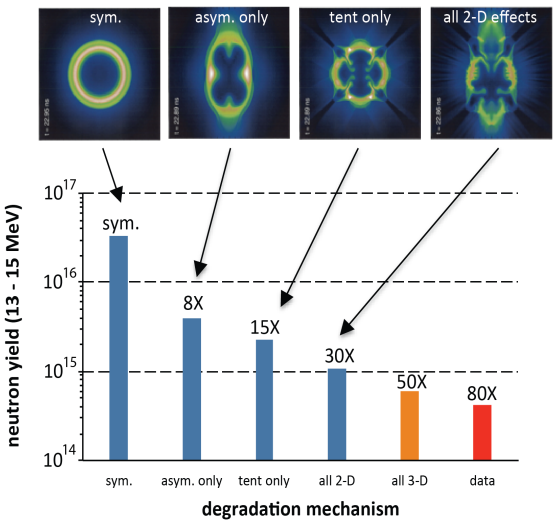

Fig. 2. Relative effect of each perturbation source in 2-D simulations of N120321.

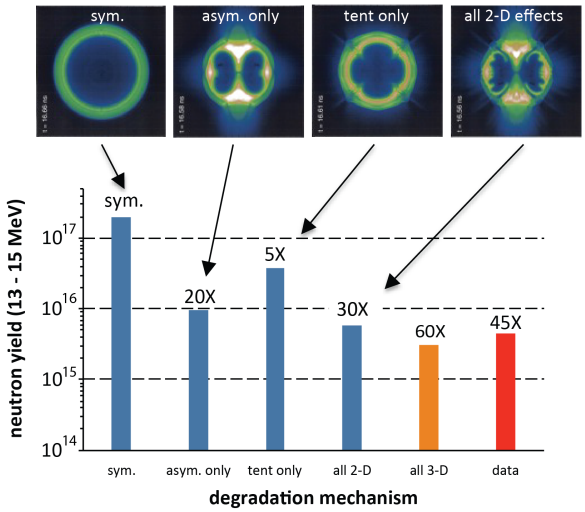

Fig. 3. Relative effect of each perturbation source in 2-D simulations of N130927.

high foot implosion N130927 is clearly much less perturbed at the ablation front. While a small tent defect is evident in this simulation, it is much reduced relative to the low foot, and the dominant perturbation source is now the hohlraum radiation asymmetry. This asymmetry results in the large spikes or jets entering the north and south poles of the hot spot in this simulation. Even so, a much larger and hotter hot spot results compared to the low foot, and hence this implosion gives a much higher yield.

To quantify the relative importance of the various perturbation sources in the low foot and high foot implosion types, Figures 2 and 3 show the results of 2-D simulations run with each perturbation source included separately, namely, the hohlraum flux asymmetries alone, the tent perturbation alone, all 2-D effects in combination, and finally the 3-D result from the simulations described above. The histogram shows the impact on the neutron yield with each effect, and the insets show the 2-D simulation results at bang time. For the low foot implosion N120321, the tent is quantitatively the largest impact resulting in a 15× yield degradation relative to 1-D. This is nearly twice the impact of the flux asymmetries that result in an 8× degradation. As shown in Figure 2, these roles reverse for the high foot. The better ablation front stability of the high foot reduces the impact of the tent to a 5× reduction in yield relative to 1-D, while the hohlraum asymmetries result in a 20× degradation. Interestingly, for the high foot, the 2-D simulation with all effects included is fairly close to the measured yield data and the 3-D simulation actually under-predicts the yield. By contrast, for the low foot, the 2-D simulation including all effects over-predicts the yield by more than a factor of two, while only the 3-D simulation is fairly close to the measured yield. This is indicative of the generally larger perturbation levels in low foot implosions that can only be accurately captured in a fully 3-D simulation.

Quantitative comparisons of the 3-D simulation results against the data for the three shots simulated are summarized in Table 1. The rows list a number of the principle experimental observables and pairs of columns compare the simulation results against the data for each successive shot. The agreement is generally good for all three shots, although many quantities are not matched within the experimental error bars. In these cases, the simulation results are generally within two error bars of the data, however. In comparing the primary neutron image size (PNI P_0), down scattered neutron image size (DSNI P_0), burn-averaged ion temperature (T_{ion}), and neutron down scattered ratio (DSR), an important caveat should be pointed out. Given the scale of these 3-D simulations, current computing capabilities do not

Table I. Comparison of simulation and experimental results for N120321, N120405, and N130927.

	N120321		N120405		N130927	
	sim.	expt.	sim.	expt.	sim.	expt.
bang time (ns)	22.85	22.91±0.04	22.53	22.70±0.08	16.53	16.59±0.03
burn width (ps)	167	158±40	130	161±40	143.5	188±30
x-ray P_0 (μm)	21.9	20.1±1.4	23.9	23.4±0.85	31.4	35.3±3.0
x-ray M_0 (μm)	19.8	22.7±2.7	24.1	26.5±4.0	45.7	49.8±1.5
PNI P_0 (μm)	24.4	26±3	25.4	27±3	27.7	32±4
DSNI P_0 (μm)	38.4	35±3	31.7	43±6	51.1	55±4
T_{ion} (keV)	2.6	3.1±0.4	1.7	1.69±0.13	3.9	4.43±0.15
DSR (%)	5.0	6.2±0.6	5.5	5.14±0.29	3.5	3.48±0.17
$Y_{13-15\ MeV}$	6.0×10^{14}	$4.2\pm0.1 \times 10^{14}$	1.4×10^{14}	$1.3\pm0.1 \times 10^{14}$	3.1×10^{15}	$4.5\pm0.1 \times 10^{15}$

allow running the simulations with inline Monte Carlo neutronics, as is routinely done in 2-D. The simulation values listed in the table are hence taken from instantaneous post-processing of the simulations at bang time. As such, they represent snapshots of the state of the simulation at bang time and omit the time averaging over the duration of the burn that is inherent in the measurement and would be included if these quantities could be computed inline. This limitation in the current simulations may account for the noticeable discrepancies in the simulated DSR for N120321 and also in the ion temperatures for N120321 and N130927. It is, of course, possible that these discrepancies point to inadequacies in the physical models used in the simulations or are the result of imperfect knowledge of the initial and boundary conditions for these shots. At this time, it is not possible to resolve which of these possibilities is responsible. Nevertheless, the overall agreement between the simulations and the data is reasonably good. This is notable given that three quite different shots have been simulated, and each appears to agree equally well with the experimental results.

Conclusions

Three ignition implosion experiments from the NIF database have been simulated following the most up-to-date 3-D simulation methodology. All three show reasonably good, though not perfect, agreement with the experimental data. Given that these three shots explored quite different regions of implosion parameter space, the agreement suggests that a fairly robust simulation capability is developing for accurately modeling the high convergence implosions being tested on NIF. This validated simulation capability is clearly essential for assessing what design modifications can lead to further gains in implosion performance.

Acknowledgments

Work performed under the auspices of the U.S. D.O.E. by Lawrence Livermore National Laboratory under Contract No. DE-AC52-07NA27344.

References

1. V. A. Smalyuk, *et al*., *Phys. Plasmas* **21** 056301 (2014)
2. B. A. Hammel, *et al*., Bull. Am. Phys. Soc. **60** 164 (2015)
3. M. J. Edwards, *et al*., *Phys. Plasmas* **20** 070501 (2013)
4. O. A. Hurricane, *et al*., *Phys. Plasmas* **21** 056314 (2014)
5. M. M. Marinak, *et al*., *Phys. Plasmas* **8** 2275 (2001)
6. D. S. Clark, *et al*., *Phys. Plasmas* **22** 022703 (2015)